1P REGULATION OF INDUCIBLE NITRIC OXIDE SYNTHASE AND CATIONIC AMINO ACID TRANSPORT BY p38α AND p38β MAP KINASES IN RAT CULTURED AORTIC SMOOTH MUSCLE CELLS

Marios Konstantinidis*, Stephen Hart#, Jiahuai Han## Michael Marber+, Jeremy Pearson+ & Anwar R Baydoun*. *Department of Biosciences, University of Hertfordshire, College Lane, Hatfield, UK. #Institute of Child Health, University College London, UK. ##The Scripps Research Institute, La Jolla, CA92037, USA. +Centre for Cardiovascular Biology & Medicine, King's College London, UK.

Previous studies suggest that induction of nitric oxide synthase (iNOS) and cationic amino acid transport (CAT) may be regulated by the p38 mitogen activated protein kinase (MAPK) pathway in cultured rat aortic smooth muscle cells (RASMC) (Baydoun *et al.*, 1999). This conclusion was based on the fact that both processes could be inhibited by SB203580, a potent inhibitor of the p38 MAPK. There is, however, growing concern over the selectivity of this compound since it also inhibits other parallel signalling pathways including the c-Jun N-terminal kinases (JNK; Clerk and Sugden, 1998). We have therefore extended our original studies by examining the effects of SB203580-sensitive isoforms of p38 on the induction of both iNOS and CATs by transfecting wild-type p38α or p38β MAPKs into RASMCs.

Briefly, RASMC isolated from male Sprague-Dawley rats (400g) were plated out in 24-well plates and allowed to grow to ~40-60% confluency before transfection with either p38α or p38β constructs in a pcDNA vector. Transfections were carried out using an integrin-binding polycationic peptide in the presence of lipofectin. Cells were activated for 24h with LPS (100 μg mL^{-1}) and IFN-γ (50 U mL^{-1}) at 3h, 6h, 12h and 24h after transfection. Production of NO was determined in the supernatant by the Griess assay. L-arginine transport was monitored as described by Baydoun *et al.* (1999).

Transfection of either p38α or p38β potentiated both NO production and L-arginine transport induced by LPS- and IFN-γ. These effects were however transient and dependent on the time of activation after transfection. Maximum potentiation of NO synthesis was observed in cells treated with LPS and IFN-γ at 6h after transfection of either p38α or p38β. Under these conditions, accumulated nitrite levels increased by 97 ± 12 % and 147 ± 16 % (n=4) respectively but declined back to the LPS and IFNγ-treated controls (0.27 ± 0.012 nmoles μg $protein^{-1}$) at 24 h. L-arginine uptake was also significantly enhanced at 6 h with both isoforms potentiating transporter activity by 418 ± 22 % and 414 ± 29 % (n=4) respectively. In contrast to the decline in NO synthesis, stimulation of L-arginine transport was sustained over 24 h post transfection. The increase in NO synthesis and L-arginine transport caused by either p38α or p38β were virtually abolished by pre-treatment of cells with 3 μM SB203580 prior to activation.

In conclusion, these findings support our previous pharmacological data and confirm that the p38 MAPK pathway is critical for the induction of both iNOS and CATs in RASMC.

Baydoun AR, Wileman SM, Wheeler-Jones CPD *et al.* (1999). Br J Pharmacol, 344, 265-272

Clerk A & Sugden PH (1998). FEBS Lett., 426, 93-96.

2P INDUCIBLE NITRIC OXIDE SYNTHASE ALONE DOES NOT ENHANCE TRANSPORT OF L-ARGININE IN HEK293 CELLS.

Zhaoqiang Cui*, Raj Tuladhar*, Stephen Hart#, Michael Marber+, Jeremy Pearson+ * Anwar R Baydoun*. *Department of Biosciences, University of Hertfordshire, College Lane, Herts, AL10 9AB, UK. #Institute of Child Health, University College London, UK. +Centre for Cardiovascular Biology & Medicine, KCL, London, UK.

We have shown previously that induction of iNOS in cultured cells is accompanied by an increase in L-arginine transport (Wileman *et al.*, 1995). It is not clear however whether this increase is independent of, or driven by, the overproduction of NO by iNOS. In a previous study we demonstrated that dexamethasone selectively blocks iNOS expression whilst having no effect on induced L-arginine transport (Baydoun *et al.*, 1993), suggesting that upregulation of transport may be independent of iNOS activity. In contrast, Hammermann *et al* (2001) have reported that inhibition of iNOS activity abolished LPS-induced L-arginine transport as a consequence of reduced L-arginine utilization by iNOS. We have therefore examined whether transient expression of iNOS results in upregulation of L-arginine transport in HEK293 cells.

HEK293 cells maintained in Dulbecco's modified Eagle's medium supplemented with 10 % foetal bovine serum were cultured to 60 % confluence in 24 well plates prior to transfecting an iNOS construct in pEGFP-N1 vector using an integrin-binding polycationic peptide plus lipofectin. Nitric oxide production was determined 48 h after transfection by the standard Griess assay. L-arginine transport was monitored in the cell monolayer as described by Baydoun *et al* (1993). Nitrite levels were undetectable in control HEK293 cells.

Transfection of iNOS gene into these cells resulted in marked NO production 48 h after transfection (Fig 1a). Under these conditions nitrite levels rose from a non-detectable value to 9.3 ± 0.5 pmoles μg $protein^{-1}$. In contrast transport of L-[^{3}H]arginine (100 μM) was unaltered at approximately 1.8 pmoles μg $protein^{-1}$ min^{-1} (Fig 1b). Transfection of cells with empty vector (EV) alone was also without effect.

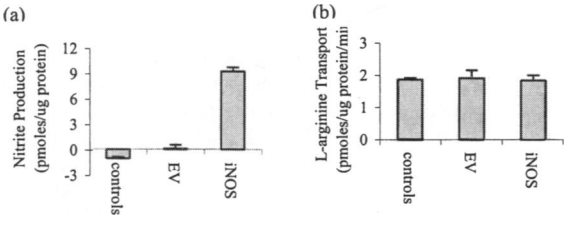

These findings suggest that upregulation of L-arginine transport under conditions of sustained NO synthesis induced by inflammatory mediators is independent of iNOS activity. Thus while enhanced L-arginine transport may be crucial for sustaining NO production, expression of iNOS alone is not sufficient to upregulate transport. This conclusion is supported by our original observations where dexamethasone blocked induction of iNOS but yet failed to modulate enhanced transporter activity.

Baydoun, A. R., Bogle, R. G., Pearson, J. D et al. (1993). Br. J. Pharmacol., **110**, 1401-1406.

Hammermann, R., Stichnote, C., Closs, E. I. et al. (2001). Br. J. Pharmacol., **133**, 379-386.

Wileman, S. M., Mann, G. E. and Baydoun, A. R. (1995). Br. J. Pharmacol., **116**, 3243-3250.

3P REQUIREMENT OF NFkB FOR THE INDUCTION OF L-ARGININE TRANSPORT IN RAT CULTURED AORTIC SMOOTH MUSCLE CELLS.

Shori Thakur, Zhaoqiang Cui, Henry Brzeski & Anwar R Baydoun. Department of Biosciences, University of Hertfordshire, College Lane, Herts, AL10 9AB, UK.

Induction of nitric oxide synthase (iNOS) in rat cultured aortic smooth muscle cells (RASMC) is accompanied by a parallel increase in L-arginine transport (Wileman *et al.*, 1999). Both processes are dependent on *de-novo* protein synthesis and can be blocked by cycloheximide. Interestingly, the glucocorticoid dexamethasone selectively inhibits iNOS expression acting, in part, by preventing the binding of NFkB to its recognition site on the iNOS promoter (Kleinert *et al.*, 1996). Thus the lack of effect of dexamethasone on induced transport would suggest that this process occurs independently of the activation of NFkB at least in RASMCs. To confirm this hypothesis we have explored the activation of NFkB and examined the effects of select inhibitors of this transcription factor on the induction of CATs in smooth muscle cells.

Confluent monolayers of RASMCs in 96-well plates were activated with bacterial lipopolysaccharide (LPS; 100 $\mu g\ ml^{-1}$) and interferon-γ (IFN-γ 100 U ml^{-1}) in the absence and presence of MG132 (a proteasome inhibitor; 0.03 μM - 3 μM), BAY 11-7082 (inhibitor of IkB phosphorylation; 0.3 μM - 30μM) or caffeic acid phenyl ethyl ester (CAPE; an inhibitor of p65 NFkB translocation; 1.0 μM - 100μM). Nitric oxide production was determined using the Griess assay. L-Arginine transport was assessed as described previously (Wileman *et al.*, 1999). In parallel studies activation of NFkB was monitored by the electrophoretic mobility-shift assay (EMSA).

Data are expressed as mean ± s.e.m. and analysed using one-way Anova followed by Dunnett's multiple comparison test.

Induced NO synthesis and L-arginine transport were both inhibited by MG132, which at 3 μM reduced accumulated nitrite levels by 80±8 % and L-arginine transport by 52±15 % respectively ($p<0.01$; n=6). CAPE was also effective in attenuating both processes, reducing NO production by 55±11 % and transport by 50±6 % at 100μM ($p<0.05$; n=6). In contrast, BAY 11-7082 was less potent against induced L-arginine transport, reducing the latter by 10±33 % ($p>0.05$) whilst inhibiting NO production by 45±12 % at 10 μM ($p<0.01$; n=6). Higher concentrations of these compounds could not be used due to their cytotoxic actions. EMSA confirmed that NFkB was activated by LPS and IFN-γ in a time-dependent manner which peaked at 2 h. This activation was either blocked or significantly inhibited by the maximum concentrations of each drug used above.

Our current data indicate that NFkB is essential, at least in part, for the induction by LPS and IFN-γ of both iNOS and transport of L-arginine in RASMC. Additional studies are however required to identify other transcriptional elements that could act in synergy with NFkB.

Kleinert, H., Euchenhofer, C., Ihrig-Biedert, I. Et al. (1996). Mol. Pharmacol., 49: 15-21.
Wileman, S.M., Mann, G.E. and Baydoun, A.R. (1995). Br. J. Pharmacol., 116: 3243-3250.

4P THE ROLE OF THE C-TERMINUS IN PROTEASE-ACTIVATED RECEPTOR-2-MEDIATED INTRACELLULAR Ca^{2+} SIGNALLING, PYK-2 ACTIVATION AND MITOGEN-ACTIVATED PROTEIN KINASE ACTIVITY.

Michael J Seatter, Robert M Drummond, Scott R Macfarlane, Toru Kanke & Robin Plevin*. Department of Physiology and Pharmacology, University of Strathclyde, John Arbuthnott Building, Glasgow G4 ONR, UK

Protease-activated receptor-2 (PAR-2) is a member of a novel family of G-protein coupled receptors, activated by serine protease-mediated cleavage of the N-terminus to generate a tethered ligand which interacts with the receptor (Macfarlane *et al.*, 2001). Human PAR-2 is activated by trypsin and the activating peptide SLIGKV. PAR-2 has been implicated in inflammation and skin development; however, little is known of the signalling events which link this receptor to these functions. Recently, we have shown PAR-2 to be linked to activation of the stress-activated protein kinases, JNK and p38 MAP kinase in a model cell system (Kanke *et al.*, 2001). In the current study we examined the role of the C-terminus in coupling of PAR-2 to these pathways and to activation of the Ca^{2+}-dependent kinase, proline-rich tyrosine kinase-2 (PYK-2).

Cloned hPAR-2 was used to create a series of deletions (D) from the extreme C-terminus; D15, D34 and D34-43. Phosphoinositide hydrolysis was measured by [^{3}H]IP accumulation, intracellular Ca^{2+} by fura-2 microfluorimetry and epitope-tagged PYK-2, JNK, p38 MAP kinase and ERK-2 activities by *in vitro* kinase assay. PAR-2 was detected by indirect immunofluorescence utilising a N-terminus antibody.

In NCTC2544 skin epithelial cells, transiently transfected with wild type (WT) hPAR-2, trypsin (30 nM) stimulated an 8-10 fold increase in [^{3}H]IP accumulation. This was not affected by D34 deletion but reduced to near basal levels in cells expressing D43, and D34-43 (see table 1).

Table 1. [^{3}H]IP accumulation in PAR-2 mutants. DPM ± s.e.m., n=4.

Mutation	WT	D34-43	D34	D43
Basal	453 ± 42	501 ± 83	443 ± 78	487 ± 87
Trypsin	2426 ± 228	685 ± 76	1907 ± 366	503 ± 61

A similar pattern was observed for increases in intracellular Ca^{2+} levels stimulated by SLIGKV (200 μM). Trypsin also stimulated the tyrosine phosphorylation of PYK-2, this was abolished in cells expressing the D34-43 mutant. Immunofluorescent staining of PAR-2 showed that D34-43 and D43 deleted also prevented trypsin-stimulated receptor internalisation. However, in contrast to the effects upon intracellular Ca^{2+} and PYK-2 activity, the D34-43 mutation had no substantial effect upon trypsin-stimulated JNK, p38 MAP kinase nor ERK activity although these responses were abolished in the D43 mutation.

The results show that a 9aa sequence within the C-terminal tail of PAR-2 is essential for coupling to the $InsP_3/Ca^{2+}$ pathway and the activation of PYK-2. However, this sequence is not essential for MAP kinase activation. Furthermore, PAR-2 internalisation is not a requirement for activation of the MAP kinases.

This work was sponsored by the MRC and BBRC.

Kanke, T., *et al.*, (2001). J. Biol. Chem. 276, 31657-31666.
Macfarlane, S. R., *et al.*, (2001). Pharmacol. Rev. 53, 245-282.

5P RESPONSE-DEPENDENT AGONIST AND INVERSE AGONIST PROPERTIES OF PROPRANOLOL AT THE HUMAN β_2-ADRENOCEPTOR EXPRESSED IN CHO-K1 CELLS

JG Baker, IP Hall & SJ Hill. Institute of Cell Signalling, Queen's Medical Centre, Nottingham NG7 2UH, UK.

We have previously reported that a variety of β_2-agonists can stimulate cyclic AMP (cAMP) accumulation and cAMP-response element (CRE) - regulated gene transcription in CHO K1 cell stably transfected with the human β_2-adrenoceptor (CHO-β_2, McDonnell et al., 1998; Baker et al., 2001a,b). We have also described how CGP 12177 can act as a partial β_2-adrenoceptor agonist on both cAMP accumulation and CRE-mediated responses (Baker et al., 2001a). In the present study we have evaluated the agonist and inverse agonist properties of propranolol, alprenolol and ICI 118551 on both cyclic AMP accumulation and CRE-mediated reporter protein (secreted placental alkaline phosphatase; SPAP) responses in these CHO-β_2 cells.

CHO-K1 cells expressing the human β_2-adrenoceptor at 300fmol/mg protein and a secreted placental alkaline phosphate (SPAP) reporter gene under the trancriptional control of six CREs (McDonnell et al., 1998) were used in the present study. Measurements of ^{3}H-cyclic AMP (cAMP) accumulation and SPAP secretion were made as described previously (McDonnell et al., 1998).

Alprenolol, acted as an agonist of both cAMP accumulation (EC_{50} 0.96 $\pm$ 0.25nM; maximum response = 1.88 $\pm$ 0.20 fold over basal; n=5) and CRE-mediated gene transcription (EC_{50} 0.28 $\pm$ 0.02nM; maximum response = 3.16 $\pm$ 0.18 fold over basal; n=5). The CRE-mediated gene transcription response was antagonised by 30nM ICI 118551 (K_D for ICI 118551 of 0.25 $\pm$ 0.03nM (n=4).

Propranolol (IC_{50} 0.70 $\pm$ 0.26nM n=3) and ICI 118551 (IC_{50} 0.81 $\pm$ 0.28nM n=3) both acted as inverse agonists of cAMP accumulation in these cells yielding a 33.7 ± 8.1% and 57.2 ± 6.8% reduction of basal cAMP accumulation. However, when CRE-mediated gene transcription was measured, propranolol acted as an agonist producing a 1.66 + 0.09 fold increase over basal SPAP secretion (EC_{50} 0.41 $\pm$ 0.11nM n=5). The agonist response to propranolol was antagonised by 30nM ICI 118551 yielding an apparent K_D for ICI 118551 of 0.14 $\pm$ 0.04nM (n=3). In contrast, ICI 118551 continued to act as an inverse agonist of CRE-mediated gene transcription in these cells.

In summary, propranolol appears able to act as both a low efficacy agonist and an inverse agonist at β_2-adrenoceptors in the same cell line in a manner that is dependent on the response being measured. These data suggest that the propranolol-induced cAMP accumulation and CRE-mediated gene transcription responses are not sequential.

JGB holds a Wellcome Trust Clinical Training Fellowship.

Baker, J.G. et al., (2001a) Br. J. Pharmacol. 134, 112P

Baker JG, et al (2001b) Bristol BPS Meeting

McDonnell J, et al (1998) Br. J. Pharmacol. 125, 717-726

6P VISUALISATION OF ADENOSINE-A_1 RECEPTORS USING THE NOVEL FLUORESCENT LIGAND, XANTHINE AMINE COGENER-BODIPY®630/650

S.J. Briddon, Y. Cordeaux, R.J. Middleton#, B. Kellam# & S.J. Hill. Institute of Cell Signalling, Medical School, Queen's Medical Centre, Nottingham, NG7 2UH. #The Pharmacy School, University Park, Nottingham, NG7 2RD.

The adenosine-A_1 receptor (A_1-AR) is a G-protein coupled receptor which is found in a variety of tissues including brain, heart, adipose tissue and muscle (Cordeaux *et al.*, 2001). By conjugating the A_1-AR antagonist xanthine amine cogener (XAC) (Jacobson *et al.*, 1986) to the fluorophore BODIPY®-630/650 (BY630), we have synthesised a fluorescent A_1-AR ligand, XAC-BY630, to allow visualisation of this receptor in living cells.

XAC-BY630 was synthesised by reacting the primary alkyl amine group of XAC with BODIPY®-630/650-X-succinimidyl ester (Molecular Probes). XAC and BY630 were stirred in N,N-dimethylformamide for 2h at room temperature and the product purified by HPLC. [^{3}H]DPCPX binding and cyclic AMP and inositol phosphate accumulation assays were performed on CHO-A1 cells as previously described (Cordeaux *et al.*, 2001). Images were acquired using a Zeiss LSM510 confocal microscope using CHO-A1 cells grown to 50% confluency on 8-well Labtek™ plates in Dulbecco's Modification of Eagle's Medium:Ham's F12 containing 5% foetal calf serum and 2mM glutamine. Cells were washed twice with HEPES-buffered saline (Dickenson & Hill, 1993), prior to incubation at 22°C with compounds as indicated.

Spectroscopic analysis of XAC-BY630 and BY630 itself showed that their peak excitation (630, 632nm, respectively) and emission wavelengths (650, 653nm) were not substantially different. [^{3}H]DPCPX binding studies on CHO-A1 cell membranes showed that XAC-BY630 had a lower affinity for the A_1-AR than XAC (pK_i=7.79±0.13 and 6.82±0.11, XAC and XAC-BY630, respectively, mean±s.e.mean, n=4). XAC-BY630 also behaved as a competitive A_1-AR antagonist at both 5'-N-ethylcarboxamidoadenosine-mediated inhibition of cAMP production (apparent pK_B=6.98±0.15 vs. 8.06±0.24 for XAC, n=3) and stimulation of inositol phosphate production (apparent pK_B=6.26±0.20 vs. 7.46±0.08 for XAC, n=4). Confocal imaging showed that XAC-BY630 bound to membrane-localised A_1-ARs in a time- and concentration-dependent manner. Binding of XAC-BY630 (25-250nM) was detected after 5 min, and was predominantly located at the membrane after a 30 min. incubation. Membrane binding of XAC-BY630 was receptor-specific, since a 30 min pre-incubation with DPCPX (10^{-8}-10^{-6}M) caused a concentration-dependent inhibition of membrane binding (30 min, 50nM).

These studies indicate that XAC-BY630 is a functional A_1-AR antagonist with moderate affinity which could be used to visualise the A_1-AR in primary tissue and cell lines.

We thank the Wellcome Trust for financial support

Cordeaux, Y., Briddon, S.J., Megson, A.E. *et al.* (2001) Mol. Pharm. 58, 1075-1084

Dickenson, J.M. & Hill, S.J. (1993) Br. J. Pharmacol. 109, 719-724

Jacobson, K.A., Kirk, K.L, Padgett, W.L. *et al.* (1986) Mol. Pharm. 29, 126-133

7P A DIFFUSIBLE SUBSTANCE MEDIATES ENDOTHELIUM-DEPENDENT CONTRACTIONS IN THE AORTA OF SPONTANEOUSLY HYPERTENSIVE RAT.

Di Yang[1], Michel Félétou[2], Nigel Levens[2], Ji Nan Zhang[1], Paul M. Vanhoutte[2]. [1]Jiangsu Province Hospital, First Affiliated Hospital of Nanjing Medical University, Nanjing 210029, China. [2]Institut de Recherches Servier, 92150 Suresnes, France.

In spontaneously hypertensive rat (SHR), the endothelium-dependent relaxation to acetylcholine (ACh) of the aorta is impaired due to the occurrence of a concomitant endothelium-dependent contraction (Lüscher & Vanhoutte, 1986). The present study was designed to determine whether or not a diffusible substance (or substances) is involved in these endothelium-dependent contractions.

Isometric tension was recorded in isolated rings or vascular strips of 35 weeks old SHR. In isolated rings and in the presence of N^G-nitro-L-arginine (L-NOARG: 100 μM), addition of tetrahydrobiopterin (BH_4: 100 μM) selectively potentiated endothelium-dependent contractions to ACh in the SHR aorta. The presence of BH_4 did not alter the characteristics of endothelium-dependent contractions i.e. involvement of oxygen-derived free radical production, cyclo-oxygenase-1 (COX-1) and TP receptors (Yang et al, 2002). A modified "sandwich"-like bioassay system was designed. Isometric tension was recorded from an aortic strip without endothelium and a donor strip, with or without endothelium, was stitched on the bioassay tissue in a way that prevented any direct contribution to the recorded contractile response. In the presence of L-NOARG and BH_4, the contractions to ACh (100 μM) occurred when the donor strip was with endothelium (300 ± 75 and 54 ± 9 mg, n = 5 for donor tissue with and without endothelium, respectively, a value of 50 mg is within the noise range of the experiment).

These contractions were abolished when the donor strip with endothelium was pre-treated with valeryl salicylate (3 mM) but remained unaffected when the assay strip was pre-treated with the preferential COX-1 inhibitor (139 ± 19, 34 ± 12 and 129 ± 37 mg, n = 7 for control, donor and recipient treated strip, respectively). Conversely, pre-treatment of the assay strip with S 18886 (5 nM) abolished the contractile response to ACh while pre-treatment of the donor strip with the TP receptor antagonist produced only a moderate inhibition (300 ± 60, 160 ± 30 and 50 ± 20 mg, n = 8 for control, donor and recipient treated strip, respectively). These endothelium-dependent contractions were not affected by the presence of superoxide dismutase (SOD: 120 Uml^{-1}) but were partially and significantly inhibited by catalase (1200 Uml^{-1}) and further inhibited by the combination of the two scavengers (220 ± 30, 220 ± 40, 130 ± 30, 80 ± 30 mg, n = 8 for control, SOD, catalase and SOD plus catalase, respectively).

These results indicate that in the SHR aorta, endothelium-dependent contractions to ACh involve a BH_4-sensitive diffusible substance and requires the activation of endothelial COX-1 and thereafter that of TP receptors situated on the smooth muscle cells.

Lüscher T & Vanhoutte PM (1986). *Hypertension,* 8, 344-348.

Yang D, Félétou M, Boulanger CM et al. (2002) *Br. J. Pharmacol.* (in press).

8P CHARACTERISATION OF THE RELAXANT RESPONSES OF EQUINE DIGITAL BLOOD VESSELS TO SUBSTANCE P

L.M. Katz, C.M. Marr & J. Elliott, The Royal Veterinary College, Royal College Street, London NW1 0TU

The factors regulating equine digital blood flow are important in understanding why horses develop digital ischaemia. Vascular sensory-motor nerves containing vasodilatory mediators, such as substance P (SP), have been detected in the equine digit. SP has been reported to cause an endothelium-dependent relaxation of equine digital arteries (EDA) and veins (EDV) (Katz *et al*, 2000). The aim of this study was to further characterise the responses of these vessels to SP.

Adjacent rings of paired endothelial-intact (+e) EDA and EDV obtained from mixed breed adult horses (n=7) killed at an abattoir were prepared for isometric tension recording (Bailey & Elliott, 1998). All vessels constricted with U44069 (9, 11-dideoxy-9alpha, 11alpha-epoxymethano-prostaglandin F2 alpha; 30 nM). The relaxant responses to carbachol (1 μM) confirmed the presence of the endothelium. The vessels were washed and some were treated with L-NAME, a NO synthase inhibitor, (N^{ω}-Nitro-L-Arginine Methyl Ester Hydrochloride; 300μM). After 20 minutes of incubation all vessels were contracted with U44069 followed by the addition of cumulative doses of SP (10^{-10}M-$3x10^{-5}$M) to obtain a concentration response curve (CRC). Relaxant responses to SP were expressed as percentage reduction in U44069 induced tone. The CRCs were fitted using computerised non-linear curve fitting. Maximal relaxation (E_{max}) was expressed as a percentage of the U44609 response. The effect of L-NAME treatment on the EC_{50} and E_{max} were made with a paired Student's *t*-test and significance set at $p \leq 0.05$.

SP produced a biphasic relaxant CRC in both EDA and EDVs, with a plateau between $3x10^{-8}$ and 10^{-7}M. Treatment of the EDAs with L-NAME resulted in almost complete inhibition of both phases of the response to SP. In comparison, a substantial L-NAME-resistant component of the both phases of the relaxant response of EDV to SP was evident. These data are presented in Table 1.

	$EC_{50}1(10^{-8}M)$	$EC_{50}2(10^{-8}M)$	E_{max1}	E_{max2}
	arithmetic mean ± sem		arithmetic mean ± sem	
Control:				
EDA	0.03 ± 0.01	24.8 ± 10.9	42.8 ± 6.3	74.9 ± 41.8
EDV	0.12 ± 0.06	15.8 ± 4.9	59.1 ± 14.4	52.0 ± 10.2
L-NAME:				
EDA	0.12 ± 0.07	8.3 ± 4.3	5.3 ± 2.5***	8.0 ± 5.2**
EDV	0.01 ± 0.003	6.8 ± 2.6	27.5 ± 12.0	15.6 ± 6.7*

*$p \leq 0.05$, **$p \leq 0.01$, ***$p \leq 0.001$ as compared to relevant control

In conclusion, SP caused biphasic concentration dependent relaxation of both EDA and EDV possibly suggesting activation of two types of tachykinin receptor. In EDA, NO appeared to mediate both phases of the response. However, in EDVs a substantial proportion of both phases of the response to SP did not appear to involve NO even though our previous studies showed the response to be entirely endothelium dependent. The role of prostacyclin and endothelium-derived hyperpolarizing factor in these responses remains to be determined.

Katz, L.M., Berhane, Y., Marr, C.M. (2000) Proc. 19th ACVIM, 889
Bailey, S.R., Elliott, J. (1998) *Equine Vet J* 130, 124-130

9P CHARACTERISATION OF NICOTINE RECEPTORS IN THE HUMAN LYMPHOCYTIC CELL LINE JURKAT

AE Summers, ME Parsons & CJ Whelan. Department of Biosciences, University of Hertfordshire, College Lane, Hatfield, Herts, AL10 9AB UK.

Studies in the literature have shown that concentrations of nicotine likely to be found in the blood of smokers (10^{-9} to 10^{-5} M), reduced interleukin-2 (IL-2) release from human lymphocytes *in vitro* (Madretsma *et al.*, 1996). Since this effect could indicate an action for nicotine on the immune system we have attempted to characterise the receptors for nicotine on the human cell line Jurkat.

Jurkat cells were cultured in RPMI medium containing 10% foetal calf serum, penicillin (50 IU ml^{-1}), streptomycin (50 μg ml^{-1}) and amphotericin B (2.5 μg ml^{-1}). RNA was extracted from Jurkat cells using a commercially available kit (QIAGEN™). In separate experiments, mRNA corresponding to the nicotinic acetylcholine receptor (nAChR) subunits alpha (α1-α7 and α10) and beta (β1-β4), using primers designed from published sources using Generunner software, was amplified by RT-PCR, separated by gel electrophoresis and visualised. Human brain RNA was also subjected to RT-PCR as a control. In functional experiments, cells were suspended in RPMI medium (10^6 cells ml^{-1}) pretreated with nicotine (10^{-12}–10^{-7}M) for 2h at 37° prior to stimulation with phorbol myristyl acetate (PMA; 25pg ml^{-1}) and phytohemagglutinin (PHA; 2.5 μg ml^{-1}) and incubation continued for a further 12h. Cell free supernatants were harvested and the IL-2 released measured by ELISA. In experiments where IL-2 release was measured dexamethasone (10^{-10}-10^{-6} M) was used as a positive control.

No mRNA for the nAChR subunits β1, β2, β3 or β4 was identified in Jurkat cells by RT-PCR. Similarly, Jurkat cells did not express mRNA for α1, α2 or α10 nAChR subunits. However, mRNA for α3, α4, α5, α6 and α7 was detected in RNA extracted from Jurkat cells.

The highest concentration of nicotine tested (10^{-7} M) reduced IL-2 release from 908.5± 83.3 pg ml^{-1} (n=3) to 880.6±104.8 pg ml^{-1} (n=3), but this reduction was not significant (P>0.05; unpaired t test). In similar experiments, dexamethasone inhibited IL-2 release, 10^{-7} M reducing IL-2 release from 693.1± 35.2 pg ml^{-1} to 440.8± 33.3 pg ml^{-1} (n=6; P<0.05).

The absence of β nAChR subunits indicates that of the α subunits present only the α7 subunit is able to form a functional receptor. However, the lack of any effect of nicotine on IL-2 release demonstrates that if such receptors are present on these cells they do not modulate IL-2 release. Thus Jurkat cells may differ from human lymphocytes studied by Madretsma *et al.*, (1996), although recent studies (Ouyang *et al.* 2000) show that higher concentrations of nicotine than those used in the present study are required to inhibit IL-2 release. Further studies are required to determine what nAChR are expressed by Jurkat cells, what aspect of cell function they modulate, and how they differ from lymphocytes.

Madretsma, GS., et al., (1996). Immunopharmacology, 35, 47-51.

Ouyang,Y., et al., (2000). *J.Allergy Clin. Immunol.*, **106**, 280-287

10P CHARACTERISATION OF THE NICOTINE RECEPTOR MEDIATING INHIBITION OF TNFα RELEASE FROM THP-1 CELLS *IN VITRO*

S. Klee, J. Bramhall, A. Vecchione, A.Sykes, M. E. Parsons & C. J. Whelan, Department of Biosciences, Faculty of Natural Sciences, University of Hertfordshire, College Lane, Hatfield, Herts, AL10 9AB.

We have previously shown that nicotine is a potent inhibitor of lipopolysaccharide (LPS) - induced tumour necrosis factor α (TNFα) release from THP-1 cells in vitro (Sykes *et al.*, 2000). THP-1 cells also contain two binding sites for nicotine, one with the properties of a nicotinic acetylcholine receptor (nAChR) and a second receptor that appears to be non-cholinergic (Morgan *et al.*, 2001). In the present communication we have used a range of compounds with activity at nAChR to characterise the receptor mediating inhibition of TNFα release.

THP-1 cells were cultured as previously described (Morgan *et al.*, 2001). Aliquots of cells (1 ml; 1 x 10^6 cells $.ml^{-1}$) were placed in 24 well plates. Cells were activated by the addition of LPS (3μg ml^{-1}) and incubated at 37°C for 4h. At the end of the incubation, the cell-free supernatent was harvested and assayed for TNFα by specific ELISA as previously described (Sykes *et al.*, 2000). Where appropriate, nicotine, epibatidine or carbachol was added to THP-1 cells 1h prior to the addition of LPS. Similarly, where hexamethonium, gallamine or α-bungarotoxin was used, these drugs were added to cells 1h prior to the addition of nicotine.

Nicotine (10^{-13}-10^{-10}M) caused a concentration-related inhibition of LPS-induced TNFα release from THP-1 cells. Concentrations of nicotine >10^{-12}M significantly (P<0.05; ANOVA) inhibited TNFα release and the highest concentration tested (10^{-10}M) reduced release from 586.9±64.6 (n=11) to 46.7±7.7 (n=6) pg.ml^{-1} a reduction of 93%.

Epibatidine (10^{-14}–10^{-10}M) and carbachol (10^{-12}–10^{-6}M) had no significant (P>0.05) effect on LPS-induced TNFα release. The highest concentrations of epibatidine and carbachol tested inhibited LPS-induced TNFα release by 21.2±6.9% (n=4) and 26.0±6.5% (n=4) respectively.

Neither hexamethonium (10^{-5}M), gallamine (10^{-6}M) nor α-bungarotoxin (10^{-6}M) significantly (P>0.05) attenuated inhibition of LPS-induced TNFα release by nicotine. However, hexamethonium enhanced the inhibition produced by 10^{-11}M nicotine decreasing TNFα release from 367.3±91.3 pg ml^{-1} in the presence of nicotine alone to 141.6±9.7 pg ml^{-1} (n=4; P<0.05) in cells treated with hexamethonium and nicotine.

We conclude that inhibition of LPS-induced TNFα release by nicotine does not appear to be mediated by nAChR that are activated by carbachol or epibatidine nor are these receptors blocked by hexamethonium, gallamine or α-bungarotoxin. However, further experiments are necessary to demonstrate that the receptor responsible is the high affinity, non-cholinergic receptor described earlier (Morgan *et al.*, 2001).

Morgan, D. *et al.*, (2001). Biochem. Pharmacol., **61**, 733-740

Sykes, A.P. *et al.*, (2000). Inflamm. Res., **49**, 311-319

11P VANILLOID RECEPTOR TYPE 1-IMMUNOREACTIVITY AND CALCIUM BINDING PROTEINS IN THE GUINEA-PIG MYENTERIC PLEXUS

A.A. Coutts & Sharon Anavi-Goffer. Biomedical Sciences, University of Aberdeen, AB25 2ZD.

Capsaicin activates a non-specific cation channel, the VR1 (vanilloid) receptor that has been cloned from rat dorsal root ganglia. Recent studies suggest that VR1-immunoreactivity occurs on neuronal fibres of the human colon (Yiangou *et al.*, 2001) and intrinsic neurones of the rat and porcine intestine. The present confocal immunohistochemical study was performed to probe the neurochemical identity and possible functional significance of VR1 in the myenteric plexus of the guinea-pig ileum and colon.

Myenteric plexus-longitudinal muscle preparations were dissected from male or female Dunkin-Hartley guinea-pigs (329-1115g) killed by cervical dislocation. Whole mount preparations were fixed with methanol at -20°C, 4% paraformaldehyde at 4°C or Zamboni's fixative at room temperature, depending on the antibody combination. Tissues were permeabilised with 1% Triton X-100 in 10% fat-free milk protein before dual-labelling with specific antibodies raised in rabbit or goat against a peptide of the predicted carboxyl terminus of the rat VR1, and against choline acetyltransferase, calretinin, calbindin, synapsin I or calcitonin gene-related peptide (CGRP). Labelling was carried out overnight at 4°C. In each experiment, at least one of the primary antibodies in the mixture was VR1 antiserum. Tissues were washed with glucose-free HBS and incubated with a mixture of the corresponding secondary antibodies for 1.5 h at room temperature. After washing with glucose-free HBS, tissues were mounted in Vectashield H-1000. Both VR1 antibodies were localised simultaneously in methanol-fixed tissues labelled with a mixture of Cy^3 donkey anti-rabbit and Alexa 488 donkey anti-goat secondary antibodies before mounting. Calretinin and CGRP antibodies were used in paraformaldehyde-fixed tissues. Control experiments included the omission of primary antibodies, the use of inappropriate secondary antibodies or preabsorption of the preparations with VR1 carboxyl terminus blocking peptide before labelling.

VR1 immunoreactivity was visualised on perikarya and fibres in both ileum and colon. An additional set of tertiary fibres, denser in the ileum than in the colon, was identified with the goat VR1 antiserum. VR1 immunoreactive neurones comprised approximately 47.1±2.81% of cholinergic cells (Mean±s.e.m.of 1079 ChAT-positive cells from 3 animals). In the ileum, calbindin is a marker for intrinsic primary afferent neurones (Dogiel type II). Approximately 67.9±2.5% of 467 VR1-positive cells from 3 animals colabelled with calbindin and nearly all calbindin-positive cells expressed VR1. Fewer VR1/calbindin-positive cells were found in the colon. Few calretinin-positive (Dogiel type I) somata expressed VR1. Some VR1-reactive fibres in the secondary plexus co-localised with CGRP whereas the tertiary fibres co-distributed with markers for calretinin and synapsin I, thus supporting an acetylcholine-releasing effect of capsaicin.

We conclude that VR1 are expressed by neuronal fibres and a variety of excitatory cholinergic ganglion cells. Subpopulations of VR1-positive cells include sensory intrinsic primary afferent neurones and CGRP-positive secreto/vasomotor neurones. The presence of VR1 on extrinsic afferent fibres cannot be excluded. VR1 expression in the myenteric plexus is clearly complex and requires further analysis particularly with techniques showing higher resolution.

Yiangou *et al*,(2001) *Lancet*, **257**, 1338-1339

12P THE EFFECT OF CANNABINOIDS ON CAPSAICIN-EVOKED CALCITONIN GENE-RELATED PEPTIDE (CGRP) RELEASE FROM THE ISOLATED HINDPAW SKIN OF DIABETIC AND NON-DIABETIC RATS.

Ruth A. Ross, Heather C. Ellington, Mary A. Cotter & Norman E. Cameron. Biomedical Sciences, Institute of Medical Sciences. Aberdeen. AB25 2ZD, Scotland.

Sensory neural dysfunction is common in patients with peripheral neuropathy, a major complication of diabetes mellitus (Cameron *et al*, 2001). A key measure of sensory neurone function is stimulus-evoked neuropeptide release. We investigated the effect of cannabinoids on capsaicin-evoked release of calcitonin gene-related peptide (CGRP) from rat paw skin *in vitro*, which is mediated by the vanilloid VR1 receptor (Kilo *et al*, 1997), comparing non-diabetic and diabetic animals. The study employed the synthetic CB_1/CB_2 receptor agonist CP55940, the endocannabinoid anandamide, which activates both CB_1 and VR1 receptors and the CB_1 receptor selective antagonist SR141716A (Pertwee, 2001).

Male Sprague-Dawley rats were 19 weeks of age when diabetes was induced by injection of streptozotocin at a dose of 40-45 $mgkg^{-1}$ i.p. After 8 weeks the animals were killed by halothane overdose. The isolated hairy skin from hindpaws was mounted onto individual glass rods which were transferred though a series of test tubes containing synthetic interstitial fluid (see Kilo *et al*, 1997) with various drug/vehicle treatments (37°C; 95% O_2 5% CO_2). Preparations remained in each tube for 10 min and then a 200µl sample of fluid was removed for measurement of CGRP levels. In some experiments, the preparations were pre-incubated with receptor agonist/antagonist/vehicle prior to exposure to capsaicin. CGRP levels were measured using a rat enzyme immunoassay kit (SPI BIO). Data are expressed as mean CGRP release in fmol per cm^2 skin ± SEM. Statistical analysis was performed using GraphPad Prism software.

Capsaicin-evoked (100µM, 0.1% DMSO) CGRP release was lower in non-diabetic than diabetic animals ($P<0.01$,unpaired t-test), being 7.06±1.80 and 16.51±2.30 $fmolcm^{-2}$ respectively (n=6). CP55940 (100nM) inhibited capsaicin-evoked CGRP release in both non-diabetic (30.92±7.69%) and diabetic animals (37.82±9.85%) compared to vehicle alone (0.1% ethanol) (n=6; $P<0.05$, paired t-test). In non-diabetic animals, the levels of capsaicin-evoked CGRP release from paw skin treated with 100nM CP55940 after incubation with 100nM SR141716A (6.13±1.04 $fmolcm^{-2}$) were higher ($P<0.05$, paired t-test) than from those treated with CP55940 after incubation with vehicle (0.1% ethanol) (3.14±0.40 $fmolcm^{-2}$) (n=6). Similarly, in diabetic animals the levels of capsaicin-evoked CGRP release from skin treated with 100nM CP55940 after incubation with 100nM SR141716A (8.03±1.21 $fmolcm^{-2}$) were higher ($P<0.05$, paired t-test) than from those treated with CP55940 after incubation with vehicle (3.41±1.28 $fmolcm^{-2}$) (n=4). Anandamide (100nM) inhibited (28.88±7.12%) capsaicin-evoked CGRP release from skin of non-diabetic animals (n=6, $P<0.05$, paired t-test), but not that of diabetic animals (4.62±12.2%) compared to vehicle alone (n=6; $P>0.05$, paired t-test). In non-diabetic animals, the levels of capsaicin-evoked CGRP release from skin treated with 100nM anandamide after incubation with 100nM SR141716A (3.17±0.68 $fmolcm^{-2}$) did not differ ($P>0.05$, paired t-test) from those treated with anandamide after incubation with vehicle (2.91±0.38 $fmolcm^{-2}$) (n=7).

The data suggest that pathological changes in the diabetic animals preclude the non-CB_1 receptor mediated inhibitory action of the endogenous cannabinoid anandamide, but not that of CP55940, which is mediated by the CB_1 receptor.

Supported by The Wellcome Trust and MRC.

Cameron N.E., *et al*, (2001). *Diabetologia*, **44**, 1973-1988.
Kilo S., *et al*. (1997). *Pain*, **73**, 201-207.
Pertwee, R.G., (2001). *Prog. Neurobiol.*,**63**, 569-611.

13P THE ENDOCANNBINOID NOLADIN ETHER ATTENUATES SENSORY NEUROTRANSMISSION IN THE RAT ISOLATED MESENTERIC ARTERIAL BED

M. Duncan, D.A. Kendall & V. Ralevic. School of Biomedical Sciences, University of Nottingham Medical School, Queen's Medical Centre, Nottingham, NG7 2UH.

Capsaicin-sensitive sensory nerves are widely distributed in the cardiovascular system (Maggi & Meli, 1988). In the mesenteric arterial bed calcitonin gene-related peptide (CGRP) is released upon activation of sensory nerves producing vasodilatation (Kawasaki *et al.*, 1988). Preliminary investigations using synthetic cannabinoids in the mesenteric bed indicate the presence of a functional cannabinoid receptor that attenuates sensory neurotransmission (Duncan *et al*, 2001). Noladin ether (NE), reported to be an endogenous cannabinoid, binds weakly to CB_1 and CB_2 receptors but exerts cannabimimetic effects *in vivo* (Hanus *et al*, 2001). The aim of the present study was to determine if this endocannabinoid mimics the actions of synthetic cannabinoids previously shown in the rat mesenteric arterial bed.

Male Wistar rats (250-300g) were killed by exposure to CO_2 and decapitation. Mesenteric beds were isolated and perfused with oxygenated Krebs' solution containing guanethidine (5μM) to block sympathetic neurotransmission (Ralevic & Kendall, 2001). After 30 min equilibration, preparations were preconstricted with methoxamine (10-100μM) and three consecutive frequency response curves to electrical field stimulation (EFS, 1-12Hz, 60V, 0.1ms, 30s) (EFS control, EFSI and EFSII) were constructed in each preparation. NE or vehicle (0.01% ethanol) was added after EFS control, 15 min before EFSI. Antagonists were added at the start of the equilibration period. In separate preparations, a dose response curve was constructed to CGRP (0.05 pmol – 0.5 nmol) in the presence of NE (1μM) and ethanol (0.01%). Data are expressed as mean±s.e.m. and analysed by ANOVA with Tukey's post hoc test or by Students unpaired t test.

EFS produced frequency-dependent relaxation (1-12Hz) of the rat mesenteric bed. Noladin ether (0.1, 1 and 3μM) attenuated sensory neurogenic relaxation evoked during EFSI and EFSII compared with EFS control in a concentration-dependent manner. In the presence of 1μM NE the response at a submaximal frequency of 8Hz was reduced from 57.33±6.83%, EFS control, to 23.30±3.78%, EFSII (n=7, $P<0.05$).

The selective CB_1 receptor antagonists LY320135 (8Hz, EFS control, 54.23±5.46% to EFSII, 18.24±3.11%, n=8, $P<0.001$) and SR141716A (8Hz, EFS control, 63.93±5.14% to EFSII, 25.19±4.36%, n=4, $P<0.01$) failed to block inhibition of the relaxation response by NE. The CB_2 receptor antagonist SR144528 also had no effect on NE-mediated inhibition. There was no significant difference between EFS control, EFSI and EFSII generated in the presence of 0.01% ethanol. NE failed to affect the response to CGRP, (pEC_{50} =10.66±0.2 and 10.5±0.1 in the presence and absence respectively of 1μM NE; $P<0.05$, unpaired t test).

These data show that NE attenuates sensory neurogenic relaxation in the rat isolated mesenteric arterial bed. The inhibitory actions of NE cannot be blocked by CB_1 and CB_2 antagonists possibly indicating that its actions are mediated by a novel receptor subtype. NE was found to have no inhibitory actions on vasorelaxation produced by exogenous CGRP indicating that the site of action is prejunctional. These results show a possible role for endocannabinoids in sensory neurogenic regulation of blood vessel tone.

We are grateful to Servier for financial support.

Duncan, M., Kendall, D.A. & Ralevic, V. (2001) *Br. J. Pharmacol.* (in press)
Hanus et al. (2001) *PNAS,* **98**, 3662-3665.
Kawasaki, H *et al.* (1988) *Nature,* **335**, 165-167.
Maggi, C.A & Meli, A., (1988) *Gen. Pharmacol.*, **19**, 1-43.
Ralevic, V & Kendall, D.A. (2001) *Eur. J. Pharmacol.*, **418**, 117-25.

14P CANNABINOIDS DECREASE INTRACELLULAR Ca^{++}AND INHIBIT LIGAND-INDUCED RISES IN $[Ca^{2+}]i$ IN AN EPITHELIAL CELL LINE (HT29)

K. Ihenetu, †D.M. Salmon, A. Molleman, M. Parsons & C.J. Whelan. University of Hertfordshire, Hatfield campus, Herts, AL10 9AB. † University of East London. London E15 4LZ.

Previously we have shown that cannabinoids inhibit TNFα-induced IL-8 secretion from HT29 cells (Ihenetu *et al.*, 2001). However the intracellular events responsible for this are presently unclear. We have studied the effects of two potent cannabinoid agonists (WIN55212-2 and CP55,940) on TNFα and acetylcholine (ACh) induced rise in $[Ca^{2+}]_i$ in HT29 cells using calcium spectrofluorimetry with Fura2/AM as $[Ca^{2+}]_i$ reporter molecule.

Adherent HT29 cells were detached (PBS/0.05% trypsin/ 0.02%EDTA), washed in McCoy 5a medium and resuspended in HEPES buffer pH 7.4 containing (10mM Glucose/1mM $CaCl_2$). Following incubation with Fura2/AM 4μM (Calbiochem-Novabiochem, Nottingham, U.K), for 45 min. at 37°C, cells were washed and resuspended in fresh HEPES. The $[Ca^{2+}]_i$ flux was measured in response to canna-binoids, TNFα and ACh on Perkin-Elmer LS5 spectrofluori-meter controlled by a desktop computer (excitation wave-lengths alternating between 340 and 380nm every 4 seconds and fluorescence fixed at 509nm). Graphical plots were prepared using commercial software (Graph Pad Prism Inc.). Calibration of each assay was performed as described by Thomas & Delaville (1982), where maximum fluorescence was measured following cell lysis with digitonin ($100\mu gml^{-1}$) and minimum fluorescence obtained with EGTA (2mM). The $[Ca^{2+}]_i$ (nM) was calculated from the equation of Grynkiewicz *et al* . (1985).

The basal $[Ca^{2+}]_i$ in HT29 cells was 171.0±17.5nM, (n=12). Addition of WIN55212-2 and CP55,940 (1 and 10μM) to HT29 cells caused a small, but significant, ($P<0.05$) concentration-related reduction in basal $[Ca^{2+}]_i$ (7.7±0.7% and 9.2±0.4%; 7.0±3.1% and 11.3±2.8%, respectively n=5) over 2min. In contrast, ACh (0.1, 1, 10 and 100μM) produced a significant ($P<0.05$) concentration-related, transient rise in $[Ca^{2+}]_i$ (11.4±2.6%, 25.3±5.8%, 48.9±9.4% and 51.9±9.2% (n=6) respectively. TNFα($100ngml^{-1}$) evoked a significant ($P<0.05$) slow increase in $[Ca^{2+}]_i$ of 33.3±3.0% over 10 min (n=5). WIN55212-2 (10μM) inhibited both ACh and TNFα induced increases in $[Ca^{2+}]_i$. WIN55212 (10μM) reduced the increase in $[Ca^{2+}]_i$ induced by ACh (10μM) (from 146.8 ± 4.5nM to 57.9±5.2nM, n=5). Similarly, WIN55212-2 (10μM) significantly ($P<0.05$) inhibited TNFα ($100ngml^{-1}$) stimulated increases in $[Ca^{2+}]_i$ (from 235.1±32.3 to 117.2±10.9nM, n=5).

We have shown that WIN55212-2 inhibits the increase in $[Ca^{2+}]_i$ induced by TNFα and ACh in HT29 cells. We suggest that the immunosuppressive effects of cannabinoids induced in HT29 may result from this reduction in resting and agonist evoked increase in $[Ca^{2+}]_i$.

Ihenetu, K., *et al.*, (2001). *Br. J. Pharmacol.*, 134, 164P
Grynkiewicz, G., *et al.*, (1985). *J. Biol. Chem.* 260, 3440-3459.
Thomas, A.P. & Delaville, F.C (1991). In *cell calcium. A practical approach*. McCormark, J.G and Cobbold, P.H. (Eds.) Oxford University Press. pp. 1-54, NY.

15P THE EFFECT OF PERIPHERAL ADMINISTRATION OF A SELECTIVE CANNABINOID CB_1 RECEPTOR AGONIST ON MECHANICALLY EVOKED RESPONSES OF SPINAL NEURONS IN ANAESTHETISED RATS.

S. Kelly & V. Chapman, School of Biomedical Sciences, University of Nottingham Medical School, Queen's Medical Centre, Nottingham, NG7 2UH.

Cannabinoid CB_1 receptors are located on the peripheral terminals of A-and C-fibre primary afferents and spinal interneurons. Non-selective cannabinoid agonists are antinociceptive when admininistered peripherally (Richardson *et al.*, 1998). Arachidonyl-2-chloroethylamide (ACEA), has been characterised as a selective CB_1 receptor agonist (Hillard *et al.*, 1999). In this study, effects of peripheral administration of ACEA on mechanical punctate-evoked responses of spinal neurons in anaesthetised rats were determined.

Extracellular recordings of convergent dorsal horn neurones were made in anaesthetised (1% halothane in 66% N_2O / 33% O_2) male Sprague Dawley rats (Chapman *et al.*, 1994). Neuronal responses to Von Frey stimulation (8, 12, 21,45 and 80g for 10secs) of the receptive field were recorded. Responses were quantified as neuronal firing rate (Hz) during a 10sec stimulus duration: Behavioural studies have demonstrated that 15g stimulation evokes reflex withdrawal in awake rats, suggesting that stimulation with >15g is nociceptive. Control responses were determined and the effects of peripheral administration of ACEA (30µg /50µl) into the receptive field on evoked responses of spinal neurons was followed for 60 minutes (n=10 rats). Data are presented as mean maximal effects and standard error of the mean; statistical analysis was performed using repeated measures ANOVA and Dunnett's *post hoc* test. Mean depths of neurons studied were 775 ± 70µm.

Mechanical punctate stimulation of peripheral receptive fields with von Frey filaments evoked an incremental increase in spinal neuronal firing (Figure 1A)

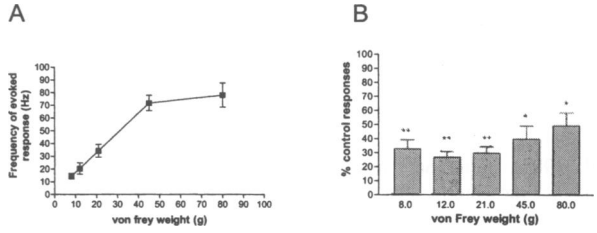

Figure 1. **A.** Control mechanical punctate-evoked responses of spinal neurons. **B.** Effect of ACEA on mechanical punctate-evoked responses of spinal neurons. *p<0.05, **p<0.01.

Peripheral ACEA (30µg/50µl) significantly reduced the 8 and 12g mechanical punctate-evoked responses of spinal neurons, similarly ACEA also significantly reduced the 12, 45 and 80g mechanical punctate-evoked responses of spinal neurons (Figure 1B).

These data demonstrate that peripheral administration of a selective CB_1 receptor agonist can inhibit spinal responses to peripheral mechanical stimulation, which correspond to the activation of A- and C-fibres.

Chapman, V., Haley, J.E. & Dickenson, A.H. (1994). *Anesthesiol.* **81**, 1429-1435.

Hillard, C.J., Manna, S. & Greenberg, M.J. (1999). *JPET.* **289**, 1427-1433.

Richardson, J.D., Kilo, S. & Hargreaves, K.M. (1998). *Pain*, **75**, 111-119.

16P (S)-AMPA INHIBITS ELECTRICALLY EVOKED CALCITONIN GENE-RELATED PEPTIDE (CGRP) RELEASE FROM THE RAT DORSAL HORN: REVERSAL BY CANNABINOID ANTAGONIST SR141716A

J.W. Brooks, A.S.C. Rice*, S.W.N. Thompson & M. Malcangio. *Pain Research, Imperial College, London, SW10, Centre for Neuroscience Research, GKT School of Biomedical Sciences, King's College, London, SE1 1UL.

In the rat spinal cord both cannabinoid receptors (CB_1) (Farquhar-Smith et al, 2000) and endocannabinoids have been identified. A CB_1 receptor-mediated inhibition of neurotransmitter release in the spinal cord has also been demonstrated in several studies. In this present study we have investigated the effect of the cannabinoid agonist WIN55,212-2 (WIN) and the selective AMPA receptor agonist (S)-AMPA on electrically evoked CGRP release from the rat spinal cord.

Male Wistar rats (200-270g) were decapitated and the spinal cords removed. Horizontal lumbar dorsal horn slices with dorsal roots (L4-L5) attached were mounted in a 3-compartment bath and superfused with Krebs' solution at room temperature (Malcangio & Bowery, 1996). Nine 8 min fractions collected; before [1-4], during [5] and after [6-9] electrical stimulation (20V, 0.5msec, 10 Hz). CGRP-like immunoreactivity (CGRP-LI) content in the concentrated perfusates was determined by specific radioimmunoassay (sensitivity 1fmol/tube). Results expressed as evoked-basal CGRP-LI release per 8-ml sample. Kruskal-Wallis one way ANOVA of ranks performed, (*p<0.05 vs control).

Basal outflow CGRP-LI from control slices was 25.4 ± 2.5 fmol/8ml fraction (mean ± s.e.m. n=8) and increased to 58.7±8.8 fmol/fraction during electrical stimulation (p<0.05). Superfusion with WIN significantly inhibited electrically evoked CGRP-LI release, and co-superfusion of SR141716A (SR1) with WIN reversed this effect (Fig. 1). (S)-AMPA superfusion inhibited the electrically evoked-CGRP-LI release compared to control, which was reversed with co-superfusion with SR1 (Fig. 1).

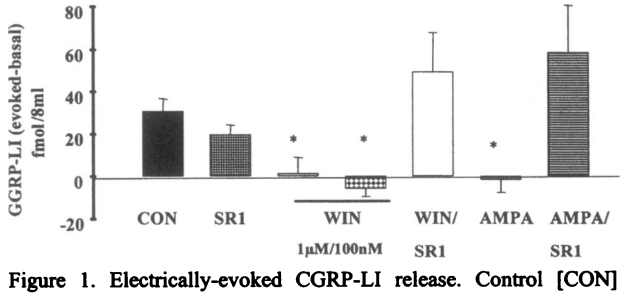

Figure 1. Electrically-evoked CGRP-LI release. Control [CON] (n=8), SR141716A 5µM [SR1] (n=8), Win55212-2 [WIN] 1µM (n=4) and 100nM (n=5), WIN 1µM + SR1 (n=6), (S)-AMPA 5µM (n=7) , (S)-AMPA 5µM + SR1 5µM(n=7).

Our data demonstrate a novel inhibition of electrically evoked CGRP release by (S)-AMPA superfusion, which is reversed by the CB_1 antagonist (SR1). AMPA inhibition may be due to the release of endogenous cannabinoids from second order neurones, acting retrogradely to inhibit the electrically evoked CGRP release.

Supported by: BJA/RCA and Wellcome Trust (MM)

Farquhar-Smith *et al.* (2000). *Mol. Cell. Neurosci.* **15**, 510-521

Malcangio M. & Bowery N.G. (1996). *Pain.* **66**, 351-358

17P THE INVOLVEMENT OF NOCICEPTIN/ORPHANIN FQ IN THE PHYSIOLOGICAL MEDIATION OF FEEDING BEHAVIOUR IN RATS

J.R. Nicholson, H. Akil & S.J. Watson (introduced by M.E. Parsons)
Mental Health Research Institute, University of Michigan, U.S.A.

Nociceptin (or Orphanin FQ, and referred to here as N/OFQ) is a 17 amino acid neuropeptide and the endogenous agonist of the ORL receptor. Central injection of N/OFQ has been shown to stimulate food intake –. an effect that may be blocked by the selective and competitive N/OFQ antagonist [Nphe^1]N/OFQ(1-13)NH_2 ([Nphe^1]) (Polidori *et al.*, 2000). In this study, we have confirmed the ability of [Nphe^1] to block N/OFQ-induced food intake, and have extended these findings to investigate the involvement of N/OFQ in the mediation of physiological feeding behaviour. Rats, being nocturnal animals, consume the majority of their daily food during the dark-phase of their diurnal cycle. We hypothesized that if endogenous N/OFQ is involved in the mediation of physiological feeding behaviour it may be expected that an N/OFQ antagonist would reduce dark-phase food intake. Therefore, we tested the effect of [Nphe^1] on dark-phase food intake in rats.

Male Sprague-Dawley rats (~250g) were anaesthetized with isoflurane, and a 22 gauge cannula was implanted into the third ventricle (3V). Coordinates from Bregma were (mm): P=0.8, L=0 and V=7.5. 3V injections were administered in a 1 µl volume over 1 minute and were separated by an interval of 2 minutes. Food intake was assessed by weight (g) and data are expressed as mean±s.e.m. For 3 or more groups, statistical analysis was carried out using One-Way ANOVA and Dunnett's post-test. For 2 groups, the Student's t-test was employed. All experiments were conducted between 08:00h and 11:00h except those investigating the effect of [Nphe^1] on dark-phase food intake – for these studies, animals were injected 0-30 minutes before the "lights-off" time (i.e. 17:30-18:00h).

At 30 minutes post 3V administration of N/OFQ (1-5nmoles) a significant increase in food intake was observed. While vehicle-treated rats consumed 0.63±0.32g of food (n=5), rats treated with 1nmole N/OFQ ate 1.77±0.18g (n=4 $p<0.05$), rats treated with 3nmoles N/OFQ ate 2.78±0.48g (n=5 $p<0.05$), and rats treated with 5nmoles N/OFQ ate 4.01±0.25g (n=4 $p<0.01$). Administration of the N/OFQ antagonist [Nphe^1] (5 or 10nmoles) before injection of 1nmole N/OFQ dose-dependently blocked the stimulatory effect of N/OFQ on food intake. At 30 minutes post-injection, rats pre-treated with saline followed by 1nmole N/OFQ consumed 2.76±0.36g (n=5), while rats pre-treated with 5nmoles N/OFQ antagonist followed by 1nmole N/OFQ ate 2.04±0.75g (n=4). Rats pre-treated with 10nmoles antagonist followed by 1nmole N/OFQ ate 0.26±0.19g (n=4, $p<0.05$).

To assess the effect of the N/OFQ antagonist [Nphe^1] on dark-phase food intake, animals were pre-treated with a cocktail of peptidase inhibitors (containing 7.5mM amastatin, bestatin, captopril and phosphoramidon) prior to injection of 30nmoles [Nphe^1], or vehicle. Food intake was measured at 1 hour, 3 hours, and 15 hours after the "lights-off" time. At 3 hours, a significant decrease in food intake was observed in the antagonist group compared with vehicle-treated controls. These rats consumed 5.93±0.60g of food (n=7), compared with 8.35±0.94g for vehicle-treated controls (n=6, $p<0.05$). Measurements taken before and after the three-hour time-point did not reveal significant differences between the groups.

In conclusion, we have demonstrated that by administering [Nphe^1] just prior to the onset of the dark-phase spontaneous feeding behaviour was significantly reduced. This, in addition to our confirmation of the ability of [Nphe^1] to block exogenously administered N/OFQ-induced food intake, suggests a role for endogenous N/OFQ in the physiological mediation of natural feeding behaviour.

Polidori, C., Calo, G., Ciccocioppo, R. *et al.*, (2000). *Psychopharmacology,* **148,** 430-437.

18P FACILITATION BY GHRELIN AND METOCLOPRAMIDE OF NERVE-MEDIATED EXCITATORY RESPONSES IN MOUSE GASTRIC FUNDUS CIRCULAR MUSCLE

C. Murray*, N. Dass A. Emmanuel* & G.J. Sanger. GI Dept., Neurology-CEDD. GlaxoSmithKline, Harlow, UK. *Dept. Physiology , St Marks Hospital, Harrow, UK.

The gastric peptide hormone, ghrelin, may stimulate gastric motility via a vagus nerve-dependent mechanism (Masuda *et al.*, 2000). This study sought to determine the effect of rat ghrelin on baseline muscle tension and nerve-mediated responses in the mouse isolated gastric fundus, comparing our findings with the effects of the gastro-prokinetic and partial 5-HT_4 receptor agonist metoclopramide (Sanger, 1998).

2 nerve-muscle strips (~3 mm wide, 10 mm long) were cut approximately parallel to the circular muscle of the gastric fundus from adult male C57Bl6/J mice (20-30 g). Each was suspended in 5 ml tissue baths under a 5 mN load for isometric recording and bathed in Krebs' solution at 37°C and bubbled with 5% CO_2 in O_2. Data acquisition and analysis were performed using Biopac Systems, Inc. MP100 hardware and AcqKnowledge software. Tetrodotoxin-sensitive (1 µM, 20 min contact, n=9 all frequencies) responses were evoked using electrical field stimulation (EFS; biphasic square-wave pulses of 0.5 ms width and maximum-effective voltage of 60-70 V) applied for 60 s every 2 min for 30 min, followed by a 10 s wash and 5 min recovery. Frequency-response data were obtained at 1, 2, 5 and 10 Hz. Data were expressed as means ± SEM and analysed using a Student's *t*-test for paired data.

At 1 and 2 Hz, EFS evoked a small atropine 1 µM-sensitive monophasic contraction. At 5 and 10 Hz, EFS evoked a triphasic response, characterised by a small, atropine-sensitive, initial contraction, followed by a relaxation and a marked post-EFS contraction. At 5 Hz, atropine 1 µM increased EFS-evoked relaxation by 164 ±61% (n=6) and reduced the after-contraction by 63 ±3% (n=3). Ghrelin and metoclopramide were applied non-cumulatively after obtaining consistent responses to 5 Hz EFS, using 30 s contact times. Ghrelin 0.01-1 µM had no effect on baseline muscle tension, but concentration-dependently facilitated the post-EFS contraction as compared to vehicle (n=5-7, $P<0.05$ each). The maximum-effective concentration was 0.1 µM (E_{max} = 43 ±15%, n=7). Metoclopramide 0.01-100 µM had no effect on baseline muscle tension but at 10-100 µM concentration-dependently facilitated the post-EFS contraction as compared to vehicle (n=5-11, $P<0.01$ each). The maximum-effective concentration was 100 µM (E_{max} = 147 ±49%, n=7). Carbachol (1 µM; submax.-effective)-induced responses were unaffected by metoclopramide 100 µM or ghrelin 0.1 µM suggesting a neuromodulatory action (n=4 each).

As demonstrated for the first time, ghrelin concentration-dependently facilitated excitatory nerve-mediated responses to EFS in mouse gastric fundus circular muscle. Despite a smaller response in comparison to metoclopramide, this effect, perhaps operating in conjunction with the vagus nerve (Masuda et al., 2000), suggests a gastro-prokinetic role for this peptide.

Matsuda Y., Tanaka T., Inomata N *et al.* (2000) Biochem. Biophys. Res. Commun., 276, 905-8.

Sanger, 1998. In: 5-HT_4 Receptors in the Brain and Periphery. Ed., Eglen RM, Springer-Verlag., pp 213-26.

19P DOWN-REGULATION OF THE 5-HT_{2A} RECEPTOR BY MIANSERIN IN RAT BRAIN IS ASSOCIATED WITH A CHANGE IN EXPRESSION OF THE IMMEDIATE EARLY GENE ARC.

T.J.R. Beveridge & J.M. Elliott. School of Pharmacy, De Montfort University, Leicester LE1 9BH

Arc (activity-regulated cytoskeleton associated protein) is an effector immediate early gene whose mRNA is selectively localised in neuronal dendrites. Its expression has been shown to be induced by neuronal stimulation and by agonist stimulation of 5-HT_{2A} receptors (Pei *et al.*, 2000). Regulation of the 5-HT_{2A} receptor is atypical in that both agonists and antagonists induce a decrease in receptor density. Mianserin is a tetracyclic antidepressant, which has shown these properties when administered both *in vitro* (Newton and Elliott, 1997) and *in vivo* (Blackshear and Sanders-Bush, 1982). The aim of the present study was to identify the functional consequences of this down-regulation induced by mianserin, as indicated by Arc mRNA expression stimulated by 1-(2,5-dimethoxy-4-iodophenyl)-2-aminopropane (DOI), a selective 5-$HT_{2A/C}$ agonist.

Male Sprague Dawley rats (190-210g) were administered (i.p.) either saline (1ml/kg) or mianserin (5 mg/kg) once per day for 2 days. This protocol has previously been demonstrated to induce 5-HT_{2A} receptor down-regulation (Blackshear and Sanders-Bush, 1982). 24 hours after the last dose of mianserin, rats were injected (i.p.) with either saline (1ml/kg) or DOI (1 mg/kg) and killed 2 hrs later. Brains were rapidly isolated and frozen in cooled isopentane and stored at -70°C prior to use. Arc mRNA expression was analysed by in situ hybridisation histochemistry using [^{35}S]-dATP labelled oligonucleotide probe as described previously (Pei et al., 2000). Relative abundance of Arc mRNA in selected areas was determined by densitometric quantification of autoradiograms using the NIH-Image system. Statistical analysis of the results was made using ANOVA with Newman-Kewls post-hoc test.

Arc mRNA expression in animals receiving mianserin followed by saline was not significantly different from saline/ saline controls in any of the brain regions measured: orbital, cingulate and parietal cortices. DOI administration following saline induced a significant increase in Arc mRNA expression in these brain regions ($p<0.05$, Table 1). Following mianserin treatment, DOI induced a significantly smaller increase in Arc mRNA expression compared to saline/DOI ($p<0.05$, Table 1).

Table 1: Effect of mianserin treatment on Arc mRNA expression levels in rat brain following DOI stimulation

Treatment	Orbital Cortex	Cingulate Cortex	Parietal Cortex
Saline/ Saline	520 ± 69	406 ± 33	253 ± 12
Mianserin/ Saline	651 ± 119	537 ± 82	282 ± 23
Saline/ DOI	1485 ± 194 *	1143 ± 138 *	961 ± 81 *
Mianserin/ DOI	1035 ± 88 *†	812 ± 78 *†	470 ± 18 *†

Values are expressed in nCi/g tissue weight as mean ± SEM for n=4-6 per group, * $p<0.05$ v Saline/ Saline, † $p<0.05$ v Saline/ DOI

Although Arc mRNA induction by DOI is acutely blocked by the 5-HT_{2A} antagonists (Pei *et al.*, 2000), the protocol used here does not generate residual tissue mianserin (Blackshear & Sanders-Bush, 1982). Therefore we conclude that 5-HT_{2A} receptor down-regulation by mianserin corresponds with a decrease in the excitatory effect of DOI on neuronal activity as revealed by Arc mRNA expression. The significance of such a functional change for the therapeutic action of antidepressants and antipsychotics remains unknown.

Blackshear MA & Sanders-Bush E (1982) *J. Pharmacol. Exp. Ther.*, **221**, 303-308
Newton RA & Elliott JM (1997) *J. Neurochem.*, **69**, 1031-1038
Pei, Q, Lewis, L, Sprakes, ME, Jones, EJ, *et al.* (2000) *Neuropharmacol.*, **39**, 463-470

20P STRUCTURAL PROPERTIES OF GROUP B LIGANDS FOR TRANSPORT-P

S. Al-Damluji* & C.R. Ganellin+, Departments of Endocrinology*, Biochemistry* and Chemistry+, University College London

Peptidergic neurones accumulate amines via an unusual uptake process designated Transport-P. Our work so far has identified two types of compounds which act as ligands for Transport-P: Group A compounds, exemplified by prazosin, are accumulated in a cooperative manner. Group B compounds, which include phenylethylamines, are accumulated non-cooperatively by the same uptake process. We studied the structural properties of this group by examining a large series of compounds for their ability to inhibit competitively the uptake of prazosin (1 uM) in immortalised gonadotrophin-releasing hormone neurones (GT1-1 GnRH cells) as previously described in detail (Al-Damluji & Kopin, 1998). All the compounds were soluble in warm DMSO at 0.1 M. The results were as follows:

1. There is an absolute requirement for an amine which is neither completely neutral nor permanently positively charged.

2. Aliphatic amines containing 1-4 carbon atoms are inactive but aliphatic amines having 5-13 carbon atoms are active. The affinity of the C10-C12 aliphatic amines for Transport-P is not much less than the affinity of their aromatic counterparts, suggesting that among compounds in this range of molecular weight, Transport-P interacts with hydrophobic amines regardless of structure.

3. Aliphatic amines consisting of a single chain of 14 or more carbon atoms are not accumulated by Transport-P. However, equivalent aliphatic compounds containing the same number of carbon atoms arranged in two chains wereactive. Transport-P cannot accumulate aliphatic amines which consist of two carbon chains if the chain lengths exceed C9. Increasing size reduced the affinity of aliphatic compounds.

4. Whereas aliphatic amines containing 18-20 carbon atoms were inactive, their aromatic counterparts desipramine (C18), imipramine (C19) and trimipramine (C20) were fully active and much more potent than smaller aromatic amines (phenylbutylamine C10; methamphetamine C10; benzylpiperidine C12).

The % efficacy (and IC50 uM) of selected compounds were: butylamine 67±4, pentylamine 95±2, hexylamine to decylamine 100, dipentylamine 94±2 (8±1.8), phenylbutylamine 92±1 (2.8±0.6), methamphetamine 94±3 (3.7±0.2), undecylamine & dodecylamine 100, dihexylamine 97±1 (3.2±1.2), MPTP 97±3 (1.1±0.3), benzylpiperidine 94±1 (4.4±0.5), tridecylamine 110±2, tetradecylamine 86±2, pentadecylamine 88±4, hexadecylamine 28±9, dioctylamine 103±3, octadecylamine -9±17, trihexylamine 90±2 (37±6), imipramine 98±2 (0.23±0.07), N-methyloctadecylamine 24±11, didecylamine 33±5.

In conclusion, Group B compounds which have the greatest affinity for Transport-P consist of a condensed cyclic structure of 18-20 carbon atoms and a basic amine which is neither completely neutral nor permanently charged. Affinity is reduced by hydroxyl groups on the aromatic ring, and increased by halogen atoms in the equivalent positions.

Al-Damluji & Kopin (1998) Brit. J. Pharmacol. 124, 693-702.

21P L-DOPA INCREASES INTRANEURONAL RELEASE OF NORADRENALINE IN RAT FRONTAL CORTEX

Lior Dayan & John P.M. Finberg. Department of Pharmacology, Rappaport Family Faculty of Medicine, Technion, Haifa 31096, Israel

L-3,4-dihydroxyphenylalanine (L-DOPA) is still the mainstay of pharmacological treatment of Parkinson's disease. Apart from its ability to readily generate dopamine (DA), however, L-DOPA may also increase noradrenaline (NA) synthesis or release. Release of NA by L-DOPA was determined: a) in isolated, electrically field-stimulated (EFS) vasa deferentia treated with yohimbine and desipramine (3 and 1 μM respectively); b) by microdialysis technique in rat frontal cortex.

Addition of L-DOPA (30 μM) to isolated vas deferens had no effect on NA released by EFS (1 Hz for 30 sec), but in tissues pretreated with AGN-1133 (N-methyl,N-propargyl,1-aminoindan; 1 μM), an inhibitor of monoamine oxidase (MAO) types A + B (Finberg *et al.*, 1981), basal overflow of NA was enhanced (from 0.76 ± 0.1 to 3.97 ± 0.4, n=5, mean ± s.e.m., P<0.001 by one way ANOVA with Tukey test). Stimulated overflow was not significantly affected.

Concentric microdialysis probes were implanted in the frontal cortex of male Sprague-Dawley rats (300-350g) under pentobarbital/chloral hydrate anaesthesia (12:60 $mg.kg^{-1}$), and microdialysate collected every 30 min at 1 μl/min the following day. L-DOPA/carbidopa (50/12.5 $mg.kg^{-1}$) was administered p.o., and amine and metabolite measurements continued for another 150 min. Microdialysate NA levels decreased to a value of 78.5 ± 11.2 % baseline at 150 min after L-DOPA/carbidopa administration (P<0.05 by comparison with control animals given water instead of L-DOPA/carbidopa), but microdialysate levels of 3,4-dihydroxyphenylglycol (DHPG) increased to 296 ± 52 % control (P<0.001). Dopamine release was enhanced, as shown by marked increases in 3,4-dihydroxyphenylacetic acid and homovanillic acid microdialysate levels (to 16 and 19 times control values respectively). In rats which were pretreated with DSP4 [N-(2-chloroethyl)-N-ethyl-2-bromobenzylamine; 50 $mg.kg^{-1}$] in order to reduce noradrenergic innervation of the frontal cortex (Jonsson *et al.*, 1981), basal microdialysate NA levels were reduced to 60% control values, and the increase in microdialysate DHPG levels caused by L-DOPA/carbidopa was prevented, although the increase in DOPAC and HVA levels was insignificantly changed. When NA reuptake was blocked locally in the perfused area of cortex by addition of desipramine (1 μM) to the perfusion fluid, microdialysate NA levels gradually increased, to 122 ± 11 % control values, and treatment with L-DOPA/carbidopa now caused an increase in microdialysate NA, to 197 ± 16 % control (P<0.001). Significance levels by two way ANOVA with Bonferroni test; n=6 for each treatment.

Although L-DOPA did not increase NA release in isolated rat vas deferens unless MAO was inhibited, in CNS neurons administration of L-DOPA/carbidopa mixture enhanced NA turnover, as shown by increased levels of the deaminated metabolite DHPG. The increased intraneuronal NA turnover may result from a displacement of vesicular NA by increased cytoplasmic DA generated from L-DOPA. The fact that extracellular NA levels were decreased by L-DOPA/carbidopa unless neuronal uptake was inhibited, may result from a reduction in physiological activity of the noradrenergic neurons at the locus coeruleus, or by a presynaptic inhibitory mechanism.

An increase in NA turnover following L-DOPA/carbidopa may result in both motor and cognitive alterations in CNS function, as well as neuroprotective activity.

Finberg JPM *et al.* (1981) *Br. J. Pharmacol.* 73, 65-74.

Jonsson G *et al.* (1981) *Eur. J. Pharmacol.* 72, 173-188.

22P ß-AMYLOID$_{25-35}$ INHIBITS GLUTAMATE UPTAKE IN CULTURED NEURONS AND ASTROCYTES: MODULATION OF UPTAKE AS A SURVIVAL MECHANISM

M.L.de Ceballos[1], B.Brera[1] & M.P.Fernández-Tomé[2]. Cajal Institute, Doctor Arce 37, 28002 Madrid, Spain; [2]Institute of Pharmacology and Toxicology, CSIC, Faculty of Medicine, UCM, 28040 Madrid, Spain.

ßAmyloid (ßA),present in senile plaques in Alzheimer's disease (AD), is considered to be important in the pathophysiology of the disease. ßA is cytotoxic to different clonal cell lines, neurons and astrocytes in culture by increasing hydrogen peroxide and altering calcium homeostasis. Interestingly, Glu transporters are exquisitely sensitive to oxidation and ßA blocks Glu uptake in astrocyte cultures (Harris *et al.*, 1996). Glu transporter proteins present in neurons and astrocytes are different. Therefore, we have studied the effect of ßA along that of dihydrokainic acid (DHK), prototype of astrocyte Glu transport inhibitors, on Glu uptake on neuron or astrocytes in culture.

^{3}H-Glu uptake was measured according to Flott & Seifert (1991) in primary astrocyte (McCarthy & de Vellis,1980) or neuronal cultures from neonatal rat or E17 fetal rat cortex. Astrocytes were plated at a density of 10^4 cells onto 96 well plates in DMEM F12/10% FCS while neurons were seeded onto 96 (toxicity, 10^5 cells) or 24 well plates (uptake, 600 x 10^3 cells) in DMEM F12/10% FCS/10% HS. Just before drug addition media was changed to defined medium. Cultures were treated with ßA$_{25-35}$ (in water to allow aggregation) or a scrambled peptide (SCR) as control. Viability was measured by the MTT assay. Glu levels in culture media were measured by reverse phase HPLC with fluorimetric detection under gradient conditions following precolumn derivatization with ophtalaldehyde. Results are the mean±s.e.m. of at least 4 independent experiments done in quatruplicate.

ßA was more potent than DHK in inhibiting Glu uptake on astrocytes (0.011 and 0.35 mM respectively) and the effect of both was less marked on neurons (0.30 and 4.56 mM, respectively). The scrambled peptide weakly inhibited uptake on astrocytes (54% at 0.25 mM) and was devoid of any effect on neurons. After 24 h exposure to ßA there was a concentration-dependent increase in Glu levels in the media from neuronal cultures. DHK only increased Glu levels at the highest concentration (Fig.1 A).

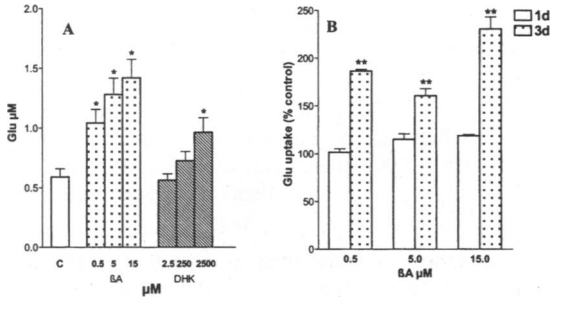

Fig.1 A. ßA increased extracellular Glu in neuronal culture media. B. Glu uptake increased at 3 days following ßA treatment of neurons. *p<0.05, **p<0.01 ANOVA followed by Student's t test.

ßA gradually (1-3 days) induced toxicity on neurons, DHK or SCR showed no effect. At 3 days following ßA exposure neurons surviving its toxic effect showed increased uptake (Fig.1, B). A similar increase was observed at 24 h on astrocytes.

In agreement with previous work (Harris *et al.*,1996) we showed that ßA not only inhibits Glu uptake in astrocytes but that it also blocks the uptake in neurons. Furthermore, this results in Glu excitotoxic levels that may be involved in the gradual toxicity of ßA to neurons in culture. Finally, increased uptake may be a survival mechanism following exposure to ßA.

Flott,B. & Seifert,W. (1991). *Glia* 4, 293-304.

Harris, M.E. *et al.* (1996). *J.Neurochem.* 67, 277-286.

McCarthy, K.D. & de Vellis,J. (1980) *J.Cell Biol.* 85,890-902.

Supported by funds from the Spanish Ministry of Education

23P BACLOFEN ALLEVIATES AKINESIA FOLLOWING INTRANIGRAL AND INTRAVENTRICULAR INJECTION IN THE RESERPINE-TREATED RAT BUT FAILS TO INHIBIT GLUTAMATE RELEASE FROM RAT NIGRAL SLICES.

T. Johnston & S. Duty. Neurodegenerative Disease Research Group, Wolfson Centre for Age-Related Diseases, King's College London, London SE1 1UL

Striatal dopamine loss in Parkinson's disease produces excess glutamate release from subthalamic efferents leading to over-activity of basal ganglia output nuclei such as the substantia nigra pars reticulata (SNr). Activation of $GABA_B$ receptors on subthalamonigral terminals may counteract this and so help to restore normal motor function. The aims of this study were to examine (i) whether $GABA_B$ receptor activation either locally (SNr) or distally (3^{rd} ventricle; 3V) alleviates akinesia in a rodent model of PD and (ii) whether $GABA_B$ receptor activation reduces glutamate release in the SNr.

Male Sprague Dawley rats (260g) were cannulated in either the SNr or 3V as previously described (Dawson *et al.*, 2000). One week later, rats received a s.c. injection of reserpine (5mg kg^{-1}). 18 hours later, when stable akinesia was obtained, rats received a single intranigral (0.5µl) or intraventricular (2.0µl) injection of the $GABA_B$ receptor agonist, baclofen (80–6000ng in PBS) or vehicle. Net increases in either contraversive rotations (SNr) or arbitrary locomotor units (ALUs; 3V) were measured for up to 90 min as an index of anti-akinetic efficacy, and the effects of different doses compared using 1-way ANOVA. The effects of pre-treatment with the $GABA_B$ receptor antagonist, CGP 46381 (2.5 µg), or vehicle on the response to consecutive doses of intranigral baclofen (800 ng) were also examined using a paired t-test.

[^{3}H]-D-aspartate release (an index of glutamate release) was measured using a two-stimulation KCl (25mM) evoked paradigm as previously described (Chadha *et al.*, 2000). Release of [^{3}H]-D-aspartate from pre-loaded rat nigral slices(350µm) was measured before (S1) and after (S2) the addition of baclofen (1-100µM) or vehicle (Krebs'). The S2/S1 ratio, a measure of release, was compared using 1-way ANOVA.

Following intranigral injection baclofen elicited a significant, dose-dependent antiparkinsonian response reaching a maximum of 162 ± 24 (mean ± s.e.m.) contraversive rotations 90 min^{-1} (n=6; $p<0.05$ versus vehicle). Intranigral CGP 46381, but not vehicle, inhibited the response to baclofen (800 ng) by 68 ± 9% (n=6; $p<0.05$). Baclofen also produced a significant reversal of reserpine-induced akinesia following intraventricular injection reaching a maximum of 543 ± 99 ALUs 80 min^{-1} (n=6; $p<0.05$ versus vehicle).

Neither vehicle nor baclofen (1–100 µM) produced any inhibition of 25 mM KCl evoked [^{3}H]-D-aspartate release from slices of rat SNr (n=5; $p>0.05$; data not shown).

The reversal of reserpine-induced akinesia seen following intranigral injection of baclofen suggests that activation of $GABA_B$ receptors alleviates SNr overactivity. Since baclofen failed to inhibit glutamate release from SNr slices it is unlikely that pre-synaptic receptors on subthalamic terminals mediate this effect. However, further clarification is needed since other reports have shown that baclofen inhibits glutamate mediated EPSPs in the SNr (Shen & Johnson, 1997). Nevertheless, that baclofen also reverses akinesia following intraventricular injection suggests that $GABA_B$ receptor agonists warrant further investigation as potential anti-akinetic treatments.

Chadha, A. *et al.*, (2000). *Br. J. Pharmacol.*, 130: 1927-1932.
Dawson, L.G. *et al.*, (2000). *Br. J. Pharmacol,*. 129: 541-546.
Shen, K.Z. & Johnson, S.W. (1997) *J. Physiol,*. 505: 153-163.

TJ is supported by an AJ Clark Studentship.

24P PHARMACODYNAMICS, CHIRAL PHARMACOKINETICS AND PK-PD MODELLING OF KETOPROFEN IN THE GOAT

P Lees, A K Arifah & M F Landoni. The Royal Veterinary College, Hawkshead Campus, North Mymms, Hatfield, Herts. AL9 7TA.

The 2-arylpropionate non-steroidal anti-inflammatory drug, ketoprofen (KTP), is a chiral compound which exists as two enantiomers, S(+) and R(-) KTP. It is licensed for use in human and veterinary medicine as the racemic mixture. It is usually classified as a non-selective inhibitor of the cyclooxygenase (COX) isoenzymes COX-1 and COX-2. The aim of this study was to generate data on the pharmacokinetics and pharmacodynamics of KTP in the goat.

KTP was administered intravenously (i.v.) to 6 goats as the racemate (3.0 mg/kg combined dose) and 6 further goats as the separate enantiomers, S(+)KTP and R(-)KTP (1.5 mg/kg of each). The racemate study was carried out as a 2-period and the separate enantiomer study as a 3-period cross-over, comparing placebo and KTP administrations. Plasma concentration-time date were used to derive pharmacokinetic variables for each enantiomer. Extravascular penetration of the drug was investigated using tissue chambers to generate inflamed (exudate) and non-inflamed (transudate) chamber fluids (Higgins *et al.*, 1984). Exudate was generated by intracaveal injection of 0.5 ml of 1% sterile carrageenan solution. *Ex vivo* inhibition of serum thromboxane (TxB_2), harvested from blood allowed to clot under standardised conditions and *in vivo* inhibition of exudate prostaglandin (PGE_2) were used tentatively as indicators of the magnitude and time course of inhibition of COX-1 and COX-2, respectively.

The pharmacokinetics of both KTP enantiomers after rac-KTP administration was characterised by rapid clearance (0.30 and 0.23 l kg^{-1} h^{-1}), short mean residence time (MRT) (1.28 and 1.36h) and low volumes of distribution at steady state (0.39 and 0.29 l kg^{-1} (Vdss) for S(+) and R(-) KTP, respectively. Area under plasma concentration-time curve (AUC) indicated slight predominance of the R(-) enantiomer (6.81 and 5.15 µg h ml^{-1}, respectively). R(-) KTP penetration into exudate and transudate was delayed but AUC values (6.00 and 5.22 µg h ml^{-1}) were only slightly less than those in plasma whilst MRT was much longer (8.84 and 6.65 h) than the corresponding plasma value. S(+) KTP penetrated less readily into exudate (AUC=2.57 µg h ml^{-1}) and transudate (too low to quantify). The separate administration of each enantiomer, revealed unidirectional inversion of R(-) to S(+) KTP.

In spite of rapid clearance and short MRT, both rac-KTP and the separate enantiomers produced marked inhibition of serum TxB_2 synthesis. This was significant ($P<0.05$) for rac-KTP and S(+) KTP up to 12 h and for R(-) KTP for 24 h. Rac-, S(+) and R(-) KTP produced moderate inhibition of exudate PGE_2 synthesis *in vivo* ($P<0.05$) for 24 h. From these data pharmacodynamic variables for S(+) KTP for inhibition of serum TxB_2 and exudate PGE_2 were calculated using the sigmoid Emax equation: Emax(%) = 94 and 100; IC_{50} (µg ml^{-1})=0.0033 and 0.0030 and N=0.45 and 0.58, respectively. The IC_{50} ratio, serum TxB_2:exudate PGE_2 was 1.10.

Higgins A J, Wright J A and Lees P (1984) *Res. Vet. Sci.*, **36**, 284-289

25P PHARMACOKINETICS, PHARMACODYNAMICS AND PK-PD INTEGRATION OF DANOFLOXACIN IN SHEEP BIOLOGICAL FLUIDS

P Lees & F Shojaee AliAbadi, The Royal Veterinary College, Hawkshead Campus, North Mymms, Hatfield, Herts. AL9 7TA, UK.

The development of resistance by microorganisms to anti-microbial drugs is a major problem in human and veterinary medicine. This has stimulated research into the selection of dosage schedules to optimise efficacy and minimise opportunities for resistance development. Danofloxacin is a synthetic antimicrobial drug of the fluoroquinolone group developed for veterinary use. It is bactericidal and acts by a concentration dependent killing mechanism (Sarasola *et al.*, 2002). For fluoroquinolones it has been demonstrated in both disease model and clinical trial investigations that, of the surrogate markers Cmax/MIC, AUC/MIC and T>MIC, outcome usually correlates with AUC/MIC and Cmax/MIC and emergence of resistance correlates with Cmax/MIC (Craig, 1998). The aim of this work was to integrate pharmacodynamic and pharmacokinetic data for danofloxacin in sheep as a means of selecting dosage schedules for evaluation in clinical trials.

Danofloxacin was administered to sheep intravenously (i.v.) and intramuscularly (i.m.) at a dose rate of 1.25 mg/kg in a 2-period cross-over study. Using subcutaneously implanted tissue chambers (Higgins *et al.*, 1984), the pharmacokinetic properties of danofloxacin were established for serum, inflamed chamber fluid (exudate) and non-inflamed chamber fluid (transudate). The acute inflammation in tissue chambers was induced by intracaveal injection of 0.5 ml of a sterile 1% carrageenan solution. For serum mean pharmacokinetic values after i.v. and i.m. dosing were, respectively: elimination half-life (3.39 and 3.17 h), volume of distribution (3.37 and 3.19 l kg^{-1}) and area under curve (1.81 and 1.68 μg h ml^{-1}). For exudate corresponding half-life values were 17.60 and 17.13 h and for transudate values were 10.45 and 17.66 h

The activity of danofloxacin in serum, exudate and transudate was established *ex vivo* and *in vitro* against a pathogenic strain of *Mannheimia haemolytica*. *Ex vivo* samples were harvested at 0,1,3,6,9,12,24,30,36 and 48 h (serum) and 0,3,6,9,12,24 and 36 h (exudate and transudate) after i.m. danofloxacin dosing. Samples were incubated for 24 h at 37°C and bacterial count determined at time 0 and 24 h. The change in bacterial count (cfu ml^{-1}) and AUC_{24h}/MIC were fitted to the sigmoid Emax equation to provide values producing bacteriostasis, bactericidal activity and elimination of bacteria. Respective values were 17.8, 20.2 and 28.7 h for serum, 20.6, 25.5 and 41.6 h for exudate and 20.9, 23.2 and 33.4 h for transudate. From the *in vivo* pharmacokinetic and *in vitro* MIC data, mean Cmax/MIC ratios of 10.8, 3.0 and 1.6 were obtained for serum, exudate and transudate after i.m. danofloxacin dosing. It is proposed that these data might be used together with MIC_{90} values for *M. haemolytica* to provide a novel approach to the design of dosage schedules.

Craig W A (1998) *Clin. Infect. Dis.* **26**, 1-10.

Higgins A J, Wright J A and Lees P (1984) *Res. Vet. Sci.* **36**, 284-289

Sarasola P, Lees P, AliAbadi F S *et al. Antimicrob. Agents Chemother.* (In press)

This work was supported by Pfizer Animal Health

26P CHARACTERIZATION OF MURINE ERG1a CHANNELS EXPRESSED IN HEK CELLS

I.A. Greenwood[1], S. Ohya[2] & B. Horowitz[2]. [1]Dept. Pharmacology & Clinical Pharmacology, St George's Hospital Medical School, London. UK. [2] Dept Physiology & Cell Biology, University of Nevada, Reno, Nevada, USA.

Recently ion channels encoded by *ether-a-go-go*-related genes (ERG) have been recorded in murine vascular smooth muscle cells (Ohya *et al.*, 2002) and RT-PCR experiments showed that only mERG1 isoforms were expressed. Various mERG1 splice variants exist (London *et al.*, 1997) and ERG channels are known to form hetero-multimers. Therefore, we investigated whether expression of mERG1a alone could underlie the native current observed in murine vascular myocytes by characterising ERG1a channels expressed in human embryonic kidney (HEK) cells. mERG1a was cloned into a neomycin-resistant pcDNA3.1 plasmid and HEK cells were stably transfected. Cells were bathed in a solution that contained 10 mM TEA, 5 mM 4-AP and 0.1 mM $CaCl_2$ with a K^+ concentration of either 5 mM or 140 mM. Ion currents were recorded in the conventional whole cell configuration using a pipette solution that contained 5 mM EGTA and 5 mM ATP. All data are the mean of n cells ± s.e.m

Activation of mERG1a channels was determined at a test potential of –100 mV following a 1 s test step to potentials between –120 mV and +60 mV from a holding potential of –60 mV. Depolarisation did not elicit large outward currents but significant inward currents were observed at the test potential. When cells were bathed in 140 mM K^+ to augment the amplitude of the current at –100 mV the potential for half maximal activation was –15 ± 6 mV (slope = 16 ± 2, n= 6).

The steady-state availability of mERG1a channels was determined at –120 mV in HEK cells bathed in a solution containing 140 mM K^+ following 5 s voltage steps from 0 mV to test potentials between –140 mV and +60 mV. The availability of the current at –120 mV was well fitted by a Boltzman function with a half-maximal availability at –87 ± 4 mV (slope = 9.7 ± 3, n= 5). The evoked current was inhibited markedly by 1 μM E4031 with a time to achieve half-maximal inhibition of 111 ± 5 s (n=5). Hyperpolarization of HEK cells bathed in 140 mM K^+-containing solution from a holding potential of 0 mV elicited currents with a distinctive hooked appearance at potentials negative to –40 mV due to the initial recovery of ERG channels from inactivation followed by deactivation. Recovery from inactivation could be described by a single exponential and was voltage dependent with the time constant increasing from 12.5 ± 0.8 ms at –120 mV to 47 ± 14 ms at –60 mV (n=5). Deactivation at –100 mV had a time constant of 381 ± 46 ms (n=4) that was considerably slower than the deactivation of native currents at the same potential (time constant = 68 ± 5 ms, n=16).

Stable transfection of HEK cells with mERG1a produced an inwardly rectifying voltage-dependent K^+ current that had kinetics of recovery from inactivation and deactivation slower than the native channel in murine vascular myocytes.

London *et al.*, (1997). *Circ Res*, **81**, 870-878

Ohya *et al.*, (2002). Manuscript submitted to *Circ Res*.